NASA Technical Memorandum 82786

Effect of Seals on Rotor Systems

David P. Fleming
Lewis Research Center
Cleveland, Ohio

Prepared for the
Fifty-second Shock and Vibration Symposium
sponsored by the Naval Research Laboratory
New Orleans, Louisiana, October 27–29, 1981

and the

Machinery Vibration Monitoring and Analysis Meeting
sponsored by the Vibration Institute
Oak Brook, Illinois, March 30–April 1, 1982

NASA

EFFECT OF SEALS ON ROTOR SYSTEMS

David P. Fleming
NASA Lewis Research Center
Cleveland, Ohio 44135

Seals can exerl large forces on rotors. As an example, in turbopump ring seals film stiffness as high as 90 MN/m (500 000 lb/in) have been calculated. This stiffness is comparable to the stiffness of rotor support bearings; thus seals can play an important part in supporting and stabilizing rotor systems. This paper reviews the work that has been done to determine forces generated in ring seals. Working formulas are presented for seal stiffness and damping, and geometries to maximize stiffness are discussed. An example is described where a change in seal design stabilized a previously unstable rotor.

INTRODUCTION

Ring seals have received considerable study over the past dozen years. The principal reason for this attention is the increasing importance of seals in affecting the dynamic response of machinery. Large forces can be generated between shafts and seals; these forces can be useful in supporting and stabilizing rotating machinery. Conversely, improperly designed seals can promote instability.

E-1121

Figure 1 illustreates a ring seal. This seal has the appearance of a journal bearing, so it is not surprising that bearing-like forces can be generated. Seals typically have larger clearances than bearings; thus hydrodynamically generated forces would be lower. (Stiffness, which equals force/displacement, changes as the inverse cube of clearance for laminar flow. Stiffness is frequently used rather than force to characterize a seal or bearing.) However, the pressure drop across a seal yields a hydrostatic force which varies directly with the pressure drop. This force can be quite large in high-pressure machinery; for example, the interstage seals of the Space Shuttle fuel pump, with a pressure drop of 140 bars (2000 psi) has a calculated stiffness of 38 MN/m (220 000 lb/in.) [1].

The purpose of this paper is to review the development of force determination in ring seals, and to present the latest, most accurate methods of calculating seal forces. Additionally, seal geometries to maximize generated forces will be discussed. An example of seal effect on rotordynamic behavior will also be presented.

SYMBOLS

A	defined by Eq. (22)
a	defined by Eq. (23)
B	seal damping coefficient
$\bar{B}$	dimensionless damping, $\frac{BC}{L^2 D \sqrt{p_o \rho}}$
$\tilde{B}$	dimensionless damping, $\frac{BC}{L^2 D \sqrt{\gamma p_o \rho_o}}$
C	radial clearance of concentric seal
$\bar{C}$	dimensionless damping, $\bar{B} \sqrt{\frac{8}{n+2}}$
D	seal diameter
E	defined by Eq. (21)
F	seal radial force
G	seal inertia coefficient
h	local seal clearance
K	seal stiffness
$\bar{K}$	dimensionless stiffness, $\frac{KC}{p_o LD}$

L	seal length
M	leakage flow
p	pressure
q	R_ω/U
R	seal radius
Re	Reynolds number, $2C\rho U/\mu$
Re_o	"sonic" Reynolds number, $2C\sqrt{\gamma p_o \rho_o}/\mu_o$
u	local fluid velocity
U	u for centered seal
V	swirl velocity
W	swirl ratio V/R_ω
x,y	transverse coordinates
z	axial coordinate
α	seal taper half-angle
γ	specific heat ratio
ϵ	eccentricity ratio e/c
η	total entrance loss factor $1 + \xi$
λ	friction factor
μ	fluid viscosity
ξ	entrance loss factor
ρ	fluid density
σ	dimensionless seal length $\lambda L/C$
ω	angular velocity

Subscripts:

0	upstream stagnation region
1	seal entrance
2	seal exit

ANALYTICAL PRINCIPLES

In the earliest analyses numerous simplifying assumptions were made. Later work removed some of these assumptions. In order to aid in understanding how a high-pressure seal operates, it is useful to go through the most elementary analysis. For this analysis the list of assumptions is, of course, the longest and reads

1. The sealed fluid is incompressible.

2. Effects of rotation are neglected.

3. Fluid flow is one-dimensional in the axial direction, that is, any circumferential flow is neglected.

4. The eccentricity is small compared with the seal concentric clearance.

5. The fluid friction factor is constant throughout the seal.

6. All flow is steady state.

7. Entrance losses can be accounted for by a suitable choice of loss coefficient.

8. There is no pressure recovery at the seal exit.

The analysis begins with the continuity and momentum equations. These are given in [2] and for invariance with time are

$$h \frac{du}{dz} = 0 \tag{1}$$

$$-\frac{1}{\rho}\frac{dp}{dz} = \lambda \frac{u^2}{h} + u\frac{du}{dz} \tag{2}$$

The boundary conditions are

$$p = p_o - \eta\rho u^2/2 \quad \text{at} \quad z = 0 \tag{3}$$

$$p = 0 \quad \text{at} \quad z = L \tag{4}$$

where η is the total entrance loss factor. It is the sum of the pressure drop, $\rho u^2/2$, that occurs due to Bernoulli's principle, and the pressure drop due to the developing velocity profile in the fluid. The value of η is 1.65 for laminar flow [3] and drops to near 1 for highly turbulent flow [4]

The solution to Eq. (1) is

$$u = \text{constant} \tag{5}$$

and to Eq. (2)

$$p = p(z = 0) - \frac{\lambda z \rho u^2}{h} \tag{6}$$

Applying the boundary conditions,

$$p_o = \rho u^2 \left(\frac{\eta}{2} + \frac{\lambda L}{h}\right) \tag{7}$$

$$p = p_o(L - z)\Big/\left(\frac{h\eta}{2\lambda} + L\right) \tag{8}$$

The total restoring force on the seal can be found by integrating the restoring component of pressure over the seal area

$$F = -R\int_0^{2\pi}\int_0^L p\cos\theta\, dz\, d\theta \qquad (9)$$

The local clearance h is given by

$$h = C(1 + \varepsilon\cos\theta) \qquad (10)$$

Invoking the small eccentricity assumption ($\varepsilon << 1$), and substituting Eqs. (8) and (10) in (9),

$$F = \pi\lambda R p_0 L^2 \eta C\varepsilon/(\eta C + 2\lambda L)^2 \qquad (11)$$

or, defining a dimensionless stiffness $\bar{K}$

$$\bar{K} = \frac{F}{\varepsilon p_0 LD} = \frac{\pi\eta\sigma}{2(\eta + 2\sigma)^2} \qquad (12)$$

where

$$\sigma = \lambda L/C \qquad (13)$$

Having derived this simple expression for seal stiffness, we can use it and the seal model to gain some understanding of how the seal develops its stiffness. Figure 2 shows the fluid pressure in the concentric seal as a function of axial distance. After an initial abrupt drop (due to the Bernoulli effect and entrance loss, Eq. (3), the pressure drops linearly to zero at the exit. The clearance and fluid velocity are uniform around the circumference.

Now consider what happens when the seal is moved to the side, Fig. 3. The clearance varies around the circumference according to Eq. (10). On the high-clearance side, the fluid can move faster than before, and, conversely, on the low-clearance side it has to go slower. The entrance pressure drop depends on the fluid velocity, so there's a greater initial drop on the high-clearance side. On both sides, the pressure must drop to zero at the seal exit. Thus the pressure profiles look like those depicted in Fig. 3. The pressure is generally higher on the low-clearance side, and this results in a force that tries to center the seal.

Figure 4 is a plot of the dimensionless seal stiffness, $\bar{K}$, versus the parameter σ which may be thought of as a dimensionless seal length. The entrance loss factor was chosen as $\eta = 1.1$, which is a value representative of turbulent flow. For low values of σ (i.e., short seals) stiffness rises with seal length. A peak is reached, and then stiffness drops as length increases. This phenomenon may be explained as follows: for very short seals, the entrance effect is the dominant pressure drop mechanism, that is, the seal behaves somewhat as an orifice. With wall friction playing such a small part, the pressure profile does not change much with seal eccentricity (see Fig. 5) and thus the stiffness is low. Conversely, for long seals wall friction causes the bulk of the pressure drop and again the pressure profile changes little with eccentricity. Thus the greatest stiffness occurs when the pressure drop due to entrance effects is comparable to that due to wall friction. This is similar to the situation in externally pressurized bearings, where for maximum stiffness the restrictor pressure drop equals the film pressure drop. To carry the analogy further, one could say that the seal entrance is analogous to the restrictor in a pressurized bearing.

A SHORT HISTORY OF ANALYTICAL DEVELOPMENT

The foundations of seal force analysis were laid by Henry Black and coworkers [5,6,7]. In keeping with the assumptions listed above, Black's analyses are one-dimensional. Essentially, Black looks at flow in a duct with a wall which moves transversely; thus the flow is unsteady. The results consist of coefficients for stiffness, damping, and inertia, such that the force on the seal is given by

$$F = Kx + B\dot{x} + G\ddot{x} \qquad (14)$$

In [6], shaft rotation is accounted for by assuming that the entire flow field rotates at one-half the shaft speed. The fluid equations are solved in a coordinate system which also rotates at half shaft speed (with fluid being assumed to flow axially in the rotating system). A coordinate transformation then yields an expression for forces on the shaft in the x and y directions

$$\begin{bmatrix} F_x \\ F_y \end{bmatrix} = -\begin{bmatrix} K - \frac{1}{4}G\omega^2 & \frac{1}{2}B\omega \\ -\frac{1}{2}B\omega & K - \frac{1}{4}G\omega^2 \end{bmatrix}\begin{bmatrix} x \\ y \end{bmatrix} - \begin{bmatrix} B & G\omega \\ -G\omega & B \end{bmatrix}\begin{bmatrix} \dot{x} \\ \dot{y} \end{bmatrix} - \begin{bmatrix} G & 0 \\ 0 & G \end{bmatrix}\begin{bmatrix} \ddot{x} \\ \ddot{y} \end{bmatrix} \qquad (15)$$

K, B, and G are the same as those for the nonrotating case. Black did, however, modify the friction factor to account for the additional fluid velocity due to rotation. For turbulent flow

$$\lambda = 0.079\left(\frac{2\rho UC}{\mu}\right)^{-1/4}\left[1 + \left(\frac{7}{16}\frac{R\omega}{U}\right)^2\right]^{3/8} \qquad (16)$$

This form was suggested by Yamada [8]. It may be noted that the mean flow velocity U is not known a priori; it must be found through iterative solutions of Eqs. (7) and (16). In [7], the circumferential variation of friction factor is accounted for; this results in a substantial increase in the direct stiffness coefficient K_{XX} (Fig. 6) but relatively small changes in the damping and inertia coefficients, compared with the constant friction factor

solution. As Fig. 6 shows, the rotational velocity affects the results; stiffness rises as rotational speed increases and, as shown in [7], damping decreases.

The works cited up to now have all used a small eccentricity analysis and presented results for small perturbations about a centered seal position. Allaire, Lee, and Gunter [2] extended the analysis to obtain results for a perturbation about a finite eccentricity position. They employed numerical integration to obtain stiffness, damping, and total load capacity for various seal eccentricities. In another departure from earlier analyses, the authors of [2] neglected the time variation of fluid velocity in the governing equations. This change simplifies the solution procedure but inevitably introduces some inaccuracy in the calculated damping coefficient (the stiffness is unaffected). In [1] this inaccuracy was found to be no more than 16 percent, with the simplified solution overestimating the damping.

The results of the finite eccentricity calculations showed that, in general, seal stiffness and damping are not much affected by eccentricity (Figs. 7 and 8). The exception is the damping in the direction of displacement, where, as would be expected, the damping coefficient increases considerably as the seal journal approaches the side wall. Seal rotation was not considered in [2].

Effect of inlet swirl. - As noted above, Black [6] accounted for seal rotation by assuming that the fluid circumferential velocity is one-half of the shaft speed throughout the seal. Actually, the fluid velocity only approaches this limit asymptotically as it proceeds through the seal. In applications such as centrifugal pump interstage seals, the fluid may enter the seal with little or no rotational velocity. Furthermore, if the seal length is short, fluid rotational speed may differ appreciably from the half-shaft-speed asymptotic value even at the seal exit. Thus seal dynamic properties are likely to vary with the amount of inlet swirl present. The effect of inlet swirl has been investigated in two papers, one by Black, Allaire, and Barrett [9] and one by Childs [10]. The analysis in [10] is the more comprehensive, as it solves the short-bearing turbulent lubrication equations of Hirs [11,12]. Since several of the assumptions listed in the Analysis section need no longer be made, it is worthwhile to list those assumptions still required by [10].

1. The sealed fluid is incompressible.

2. Pressure-induced circumferential flow is neglected (the "short bearing" approximation [13]).

3. The eccentricity is small compared with the seal concentric clearance.

4. Entrance losses can be accounted for by a loss coefficient.

5. There is no pressure recovery at the seal exit.

Childs results [10] for direct and cross-coupled stiffness and damping are given for turbulent flow by

$$K_{xx} = K_{yy} = \frac{\pi\sigma}{n + 2\sigma}\left\{1.25E - \frac{1}{\sigma}\left(L\,\frac{q}{D}\right)^2\left\{\frac{1 + 6E}{12} + \frac{2W_1 - 1}{a}\left[\left(E + \frac{1}{a^2}\right)(1 - e^{-a}) - \left(\frac{1}{2} + \frac{1}{a}\right)e^{-a}\right]\right\}\right\} \tag{17}$$

$$K_{xy} = -K_{yx} = \frac{\pi\sigma L\Omega}{D(n + 2\sigma)}\left\{\frac{E}{\sigma} + \frac{A}{12}(1 + 6E) + \frac{2W_1 - 1}{a}\left\{AE + \left(\frac{1}{\sigma} - \frac{A}{a}\right)\left[(1 - e^{-a})\left(E + \frac{1}{2} + \frac{1}{a}\right) - 1\right]\right\}\right\} \tag{18}$$

$$B_{xx} = B_{yy} = \frac{\pi c}{\sqrt{2}(n + 2\sigma)}\left[\frac{E}{\sigma} + \frac{A}{12}(1 + 6E)\right] \tag{19}$$

$$B_{xy} = -B_{yx} = \frac{\sqrt{2}\pi L\sigma}{D\sqrt{n + 2\sigma}}\left\{\frac{1 + 6E}{12} + \frac{2W_1 - 1}{2a}\left[(1 - e^{-a})\left(E + \frac{1}{2} + \frac{1}{a^2}\right) - \frac{1}{2} - \frac{e^{-a}}{a}\right]\right\} \tag{20}$$

$$E = \frac{n}{2(n + 6\sigma)} \tag{21}$$

$$A = 1 + \frac{3}{q^2 + 4} \tag{22}$$

$$a = \sigma\left(1 + \frac{0.75\,q^2}{q^2 + 4}\right) \tag{23}$$

Also, q is defined as the ratio of journal rotational speed to mean axial velocity,

$$q = \frac{R\omega}{U} \tag{24}$$

The initial swirl ratio W_1 is the ratio of circumferential fluid velocity at the seal entrance to the journal speed,

$$W_1 = \frac{V_1}{R\omega} \tag{25}$$

The swirl ratio approaches 1/2 as the fluid proceeds through the seal; W_1=1/2 implies the half-journal speed assumption of Black and Jenssen [6].

While the expressions above appear complicated, they can be programmed on a pocket calculator or digital computer in a straightforward manner. Figure 9 shows the results of the calculations. The seal used for these calculations has a length to diameter ratio of 1/2; the circumferential journal speed is 1/2 that of the mean axial fluid velocity.

As expected, preswirl has a stronger effect for small values of σ, the dimensionless seal length. The larger the initial value of circumferential fluid velocity, the smaller is the direct stiffness and the larger the cross-coupled stiffness and damping, while direct damping is completely unaffected. Cross-coupled stiffness is usually viewed as promoting instability. Small values of preswirl reduce K_{xy} and thus would appear to be stabilizing. The authors of [9] point out that negative preswirl - the fluid revolving opposite the direction of shaft motion - can result in negative K_{xy} and thus counteract whirl-producing forces elsewhere on the shaft.

State of the art. - This term is used with some misgivings, as ring seals continue to received intensive study and new publications appear frequently.

Equations (17) to (20) presented above appear to be the most comprehensive available to calculate seal stiffness and damping, requiring the fewest simplifying assumptions and presenting results in explicit form. Results are limited to small displacements from the centered position, but, as shown in [2], seal stiffness and damping are largely insensitive to seal eccentricity. The source of Eqs. (17) to (20), [10], also presents expressions for inertia coefficients, but these are usually of minor importance.

Recently two authors have investigated seals of finite length (thereby eliminating the short seal assumption). In [14] the turbulent Reynolds equation was solved numerically for finite eccentricity ratios, using the finite element method. Childs, in [15], starts with Hirs' bulk flow equations [11,12], transforms them to ordinary differential equations by small eccentricity assumptions, and integrates numerically. Both references report that the short seal solution overestimates the seal coefficients with the error increasing for longer (L/D) seals.

In this connection, Black and Jenssen [6] proposed correction factors for finite length seals based on an approximate analysis. The results of [14] and [15] indicate that these factors result in overcorrection. A more accurate formula would seem to be

$$\begin{Bmatrix} K \\ B \end{Bmatrix}_{finite} = \begin{Bmatrix} K \\ B \end{Bmatrix}_{short} \frac{1}{1 + 0.6\left(\frac{L}{D}\right)^2}$$

EXPERIMENTAL CORRELATION

Experimental data, particularly dynamic data, are very sparse. Black and Jenssen show results of experiments in [6] and [7] for axial Reynolds numbers up to 20 000 and rotational Reynolds numbers (based on half journal speed) up to 14 000. Both unidirectional and rotating load (due to unbalance) tests were run. In both papers, agreement between analysis and experiment is shown as close, although the analysis of [7] employed the local friction factor effect while that of [6] did not. Childs and Dressman [16] have presented preliminary results which show that measured direct stiffness is generally a good deal higher than predicted by [10] (to 90 percent) while direct damping is much lower than predicted.

OPTIMUM GEOMETRIES

Thus far it has been tacitly assumed that the seal clearance is constant in the axial direction; in other words the seal has a straight bore. From physical reasoning it is easy to see that the direct stiffness would be higher if the clearance at the fluid exit were less than at the entrance. In [17] Fleming calculated stiffness for seals with stepped and tapered bores (Fig. 10) and determined optimum geometries to maximize either the stiffness K on the ratio of stiffness to leakage K/M. This was followed with calculations for damping in tapered bore seals [1]. Figure 11 shows that substantial increases in stiffness are possible with an optimum taper configuration. The stiffness increase is obtained with only a moderate leakage penalty. The inlet-to-outlet clearance ratio for the maximum K/M seal is nearly constant over the entire range of dimensionless seal lengths (σ) shown in Fig. 11 having a mean value of 1.9. Direct damping is lower in tapered seals as shown in Fig. 12. This is principally because of the tapered seals larger average clearance (tapered and straight bore seals are compared using the minimum clearance in the seal). More recently Childs extended his solution of Hirs' lubrication equations to tapered bore seals [18]. His results agree qualitatively with those of [1] and [17]. Childs considers variable inlet swirl and rotational effects within the constraint of the short bearing approximation; thus greater accuracy would be expected.

SEALS FOR COMPRESSIBLE FLUIDS

The flow of a compressible fluid (most commonly a gas) differs from that of an incompressible fluid in that changes in pressure are accompanied by changes in pressure and temperature. For flow through a seal - usually approximated as adiabatic - as the pressure drops along the flow path the density and

temperature also drop, and the velocity increases. Except for the special case of a converging-diverging channel, the maximum fluid speed is limited by the speed of sound. Thus for some ratio of upstream to downstream pressure the flow will become choked and hence unaffected by further decreases in downstream pressure.

Fluid compressibility has a large effect on the forces generated in seals. Stiffness and damping coefficients are calculated for both straight bore and tapered-bore seals in [4] and [19]. All of the assumptions listed in the analysis section apply, except, of course, that compressibility is allowed; the fluid is assumed to be a perfect gas. Figure 13 shows stiffness of straight seals and optimum tapered seals for choked flow. The abscissa is the seal clearance-to-length ratio C_2/L times a Reynolds number Re_0 formed using the speed of sound for conditions upstream of the seal.

$$Re_0 = 2C\sqrt{\gamma p_0 \rho_0}/\mu_0$$

The curves on the left are for laminar flow. The nearly horizontal curves on the right are for turbulent flow; there is a separate curve for each value of C_2/L. The left end of the curves for turbulent flow corresponds to a Reynolds number in the seal passage of 3000; this is generally considered the lowest value for which one can be assured of turbulent flow. A Reynolds number of 2300 is usually taken as the upper limit for laminar flow. Points where Re = 2300 are shown for various C_2/L values on the laminar flow curves.

The surprising feature of the results is the negative stiffness predicted for low values of C_2/L. This is analogous to the lockup phenomenon observed in pressurized gas-lubricated bearings. Negative stiffness could cause rapid failure of floating ring seals and would rarely be beneficial even for rigidly mounted seals. Tapered seal stiffness is always positive and generally much higher than straight seal stiffness. The optimum clearance ratio is near 1.9 for most conditions, as it is for incompressible fluids.

Damping is shown in Fig. 14. As for stiffness, laminar flow curves are on the left and turbulent-flow curves (a separate one for each C_2/L) are on the right. Again, as for incompressible fluids, damping is lower for tapered seals. Damping is minimized for clearance-to-length ratios of 0.002-0.005 and is higher for ratios outside this range.

Expermental data are again sparse. Hendricks [20] obtained pressure measurements along the length of straight and tapered bore seals in the concentric and fully eccentric positions. Because of the small number of pressure taps he did not attempt to determine a net force generated by the seal; however, he estimated that the overall stiffness of the tapered seal was no higher than that of the straight seal. Physical reasoning leads one to question this conclusion.

In work by Burcham and Diamond [21] the tapered bore seal was far superior to an alternative seal, a Rayleigh lift pad design. Both were floating ring seals, and the objective was to determine the endurance of the seals while maintaining satisfactory leakage control (i.e., minimizing wear). No internal pressure measurements or force measurements were made. In this type of test, the seal having a higher stiffness (higher centering force) can better minimize the rubs which cause wear. The investigators noted that there was less seal wear when sealed pressure was higher. This is in agreement with the analysis, which shows that a higher sealed pressure produces higher seal stiffness.

SEAL EFFECT ON ROTOR DYNAMICS

When significant forces (or equivalently, stiffnesses) are generated by seals, the effect on the shaft-rotor system is the same as if a bearing of that stiffness were placed on the shaft. Consequently, changes in dynamic response can be expected as a function of seal stiffness.

An example of seal forces being exploited to favorably influence rotor dynamic response is the high pressure fuel pump for the space shuttle main engine. The rotor of this pump is shown schematically in Fig. 15. Three centrifugal pump stages are driven by a two-stage axial turbine. The rotor is supported on two duplex ball bearings. Ring seals are used between pump stages. Originally, these seals were of serrated design (Fig. 16) to deliberately reduce the forces produced, as it was believed the cross-coupled stiffness would promote instability. In fact, other exciting forces produced a subsynchronous instability which began as the pump speed passed twice the first critical speed. Various modifications were tried to eliminate the instability. There was little success until the serrated seals were replaced with smooth-bore seals [22]. With this change the pump could be run to full speed without exhibiting signs of instability. The conclusion drawn was that the higher direct stiffness of the smooth seals was largely responsible for the stabilization and that the benefit of higher direct stiffness overshadowed the deleterous effect of the higher cross-coupled stiffness. The effect of higher-stiffness seals can be quantified in one respect by determining the effect on resonances. This is shown in Fig. 17 where resonant frequency is plotted as a function of interstage seal stiffness for a rotative speed of 37 000 rpm, the normal operating speed. The stiffness of the original serrated seals is not known precisely; however seal stiffness has little effect on resonant frequency for low values of stiffness. The first and second resonances are 9500 and 19 800 cpm,

respectively. When the serrated seals are replaced by smooth-bore seals, the resonances have risen to 13 500 and 23 000 cpm. Further increases occur if optimum tapered-bore seals, described earlier, are used. The two resonances then are 16 000 and 28 000 cpm. These frequencies are 70 and 40 percent higher, respectively, than the resonant frequencies with the original serrated seals.

CONCLUDING REMARKS

Significant forces can be generated by ring seals; film stiffnesses as high as 90 MN/m (500000 lb/in.) have been calculated for turbopump ring seals. These forces have been effectively utilized to support and stabilize shaft-rotor systems. This paper has presented a summary of work that has been done to determine forces generated in ring seals. Both compressible and incompressible fluids were considered; working formulas were presented to calculate seal stiffness and damping. Seal geometries to maximize stiffness were described. An example showed the effect seals can have on the dynamic behavior of rotor systems; use of high-stiffness seals raised the rotor critical speeds by nearly 50 percent.

REFERENCES

1. David P. Fleming, "Damping in Tapered Annular Seals for an Incompressible Fluid." NASA TP-1646, 1980.

2. P. E. Allaire, C. C. Lee, and E. J. Gunter, "Dynamics of Short Eccentric Plain Seals with High Axial Reynolds Number." J. Spacecraft, Vol. 15, No. 6, Nov.-Dec. 1978, pp. 341-347.

3. D. P. Fleming and E. M. Sparrow, "Flow in the Hydrodynamic Entrance Region of Ducts of Arbitrary Cross Section." J. Heat Transfer, Vol. 91, Aug. 1969, pp. 345-354.

4. David P. Fleming, "Stiffness of Straight and Tapered Annular Gas Path Seals." J. Lubrication Technology, Vol. 101, No. 3, July 1979, pp. 349-355.

5. H. F. Black, "Effects of Hydraulic Forces in Annular Pressure Seals on the Vibration of Centrifugal Pump Rotors." J. Mechanical Engineering Science, Vol. 11, No. 2, 1969, pp. 206-213.

6. H. F. Black and D. N. Jenssen, "Dynamic Hybrid Bearing Characteristics of Annular Controlled Leakage Seals." Proc. Inst. Mech. Engineers, Vol. 184, Part 3N, 1969-1970, pp. 92-100.

7. H. F. Black and D. N. Jenssen, "Effects of High Pressure Ring Seals on Pump Rotor Vibrations." ASME Paper 71-WA/FE-38, Nov. 1971.

8. Yutaka Yamada, "Resistance of a Flow through an Annulus with an Inner Rotating Cylinder." Bulletin of JSME, Vol. 5, No. 18, 1962, pp. 302-310.

9. H. F. Black, P. E. Allaire, and L. E. Barrett, "Inlet Flow Swirl in Short Turbulent Annular Seal Dynamics." Presented at Ninth Int. Conf. on Fluid Sealing, BHRA Fluid Engineering, Leeuwenhorst, Netherlands, 1981.

10. D. W. Childs, "Dynamic Analysis of Turbulent Annular Seals Based on Hirs' Lubrication Equation." To be published in J. Lubrication Technology.

11. G. G. Hirs, "Fundamentals of a Bulk-Flow Theory for Turbulent Lubricant Films." Doctoral Thesis, Delft Univ. Technology, 1970.

12. G. G. Hirs, "A Bulk-Flow Theory for Turbulence in Lubricant Films." J. Lubrication Technology, Vol. 95, No. 2, April 1973, pp. 137-146.

13. George B. DuBois and Fred W. Ocvirk, "Analytical Deviation and Experimental Evaluation of Short-Bearing Approximation for Full Journal Bearings." NACA Rep. 1157, 1953.

14. Richard H. Schmaus, "Static and Dynamic Properties of Finite Length Turbulent Flow Annular Seals." MS Thesis, Univ. Virginia, 1981.

15. D. W. Childs, "Finite Length Solutions for Rotordynamic Coefficients of Turbulent Annular Seals." Submitted to J. Lubrication Technology.

16. Dara W. Childs, John B. Dressman, and S. Bart Childs, "Testing of Turbulent Seals for Rotordynamic Coefficients." Paper in Rotordynamic Instability Problems in High Performance Turbomachinery, NASA CP-2133, 1980, pp. 121-138.

17. D. P. Fleming, "High Stiffness Seals for Rotor Critical Speed Control." ASME Paper 77-DET-10, 1977.

18. D. W. Childs, "Convergent-Tapered Annular Seals: Analysis for Rotordynamic Coefficients." Symposium volume, Fluid/Structure Interactions in Turbomachinery, ASME Winter Annual Meeting, 1981, pp. 35-44.

19. David P. Fleming, "Damping in Ring Seals for Compressible Fluids." Paper in Rotordynamic Instability Problems in High Speed Turbomachinery, NASA CP-2133, 1980, pp. 169-188.

20. R. C. Hendricks, "Some Flow Characteristics of Conventional and Tapered High-Pressure-Drop Simulated Seals." ASLE Transactions, Vol. 24, No. 1, pp. 23-28, 1981.

21. R. E. Burcham and W. A. Diamond, "High-Pressure Hot-Gas Self-Acting Floating Ring Shaft Seal for Liquid Rocket Turbopumps." NASA CR-165392, 1980.

22. Matthew C. Ek, "Solving Subsynchronous Whirl in the High-Pressure Hydrogen Turbomachinery of the SSME." J. Spacecraft, vol. 17, no. 3, 1980, pp. 208-218.

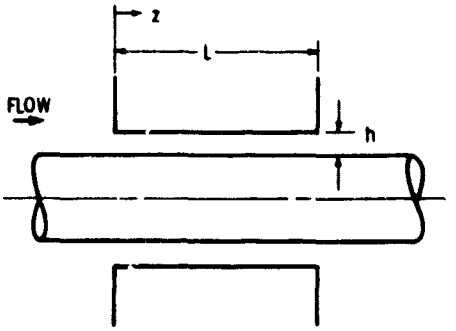

Figure 1. - Ring seal.

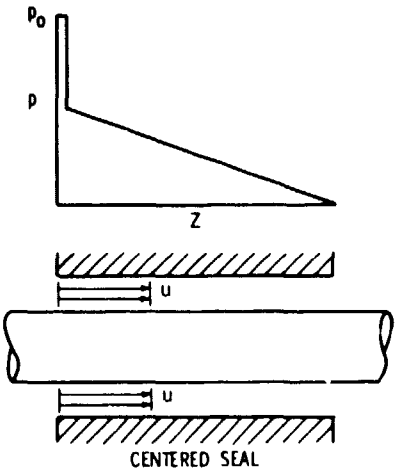

Figure 2. - Velocity and pressure profile in concentric seal.

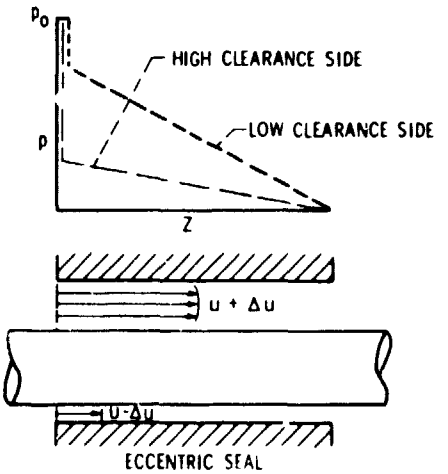

Figure 3. - Velocity and pressure profile in eccentric seal.

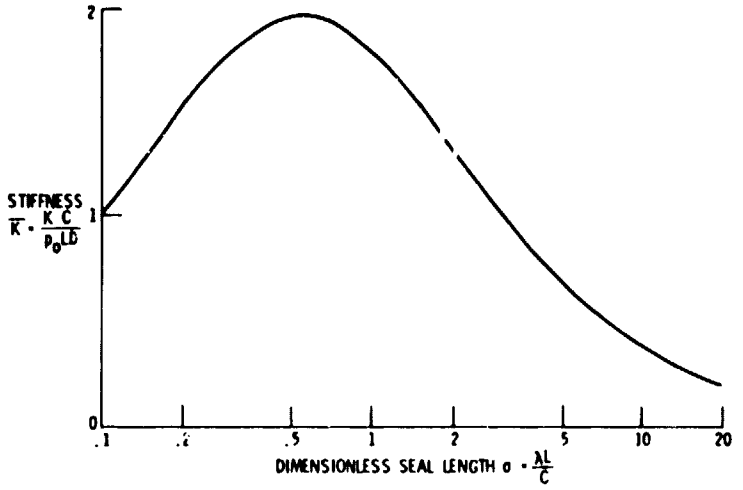

Figure 4. - Ring seal stiffness.

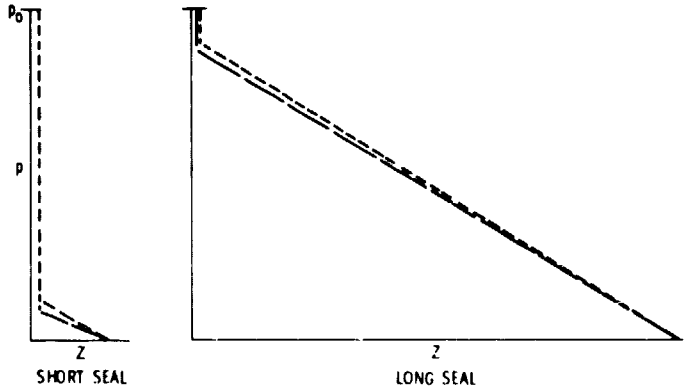

Figure 5. - Pressure profiles in short and long seals.

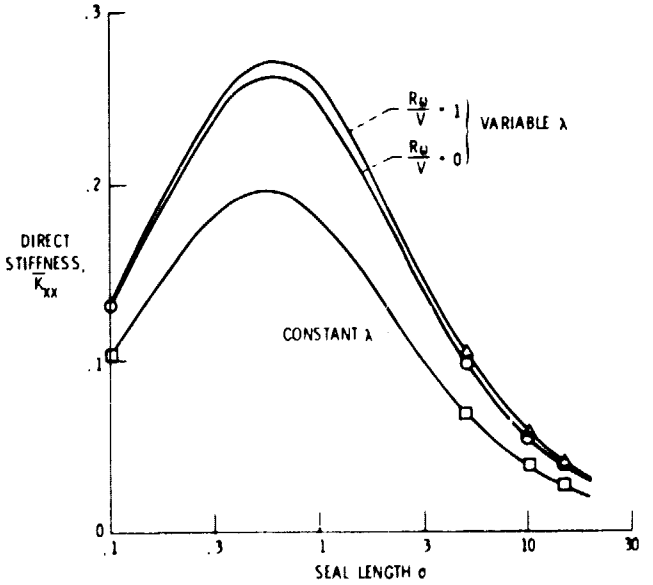

Figure 6. - Increase in stiffness due to effect of local Reynolds number on friction factor

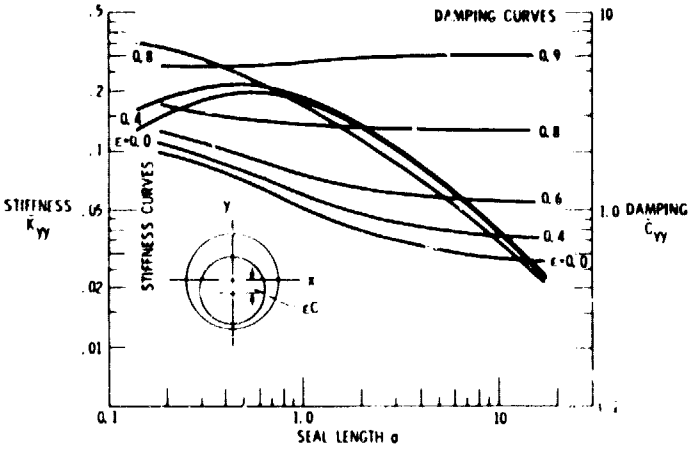

Figure 7 - Seal stiffness and damping in line with journal displacement (from [21]).

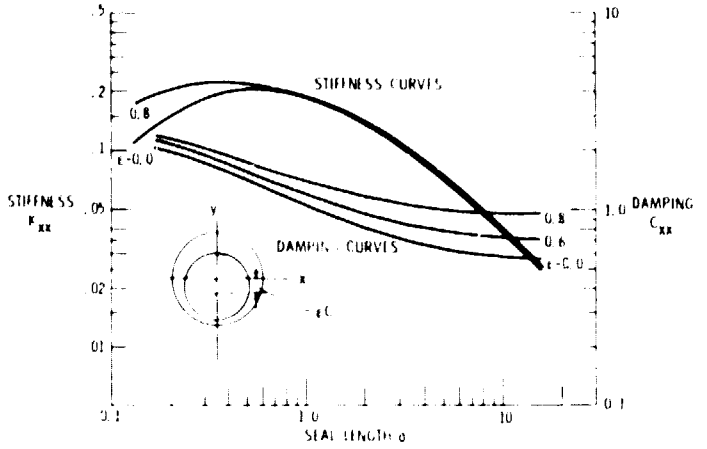

Figure 8 - Seal stiffness and damping normal to journal displacement (from [21]).

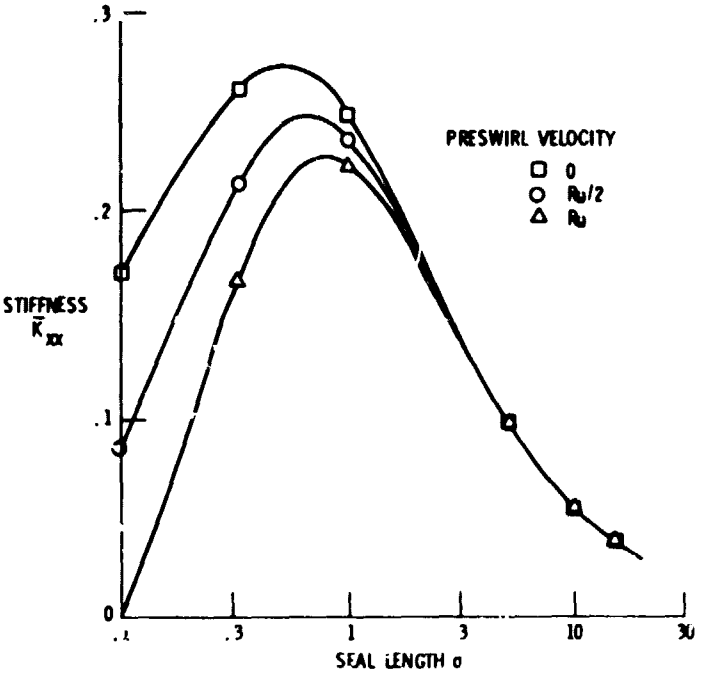

(a) Direct stiffness.

Figure 9. - Effect of preswirl on dynamic seal coefficients; L/D = .05, $R\omega/u_0$ = .05.

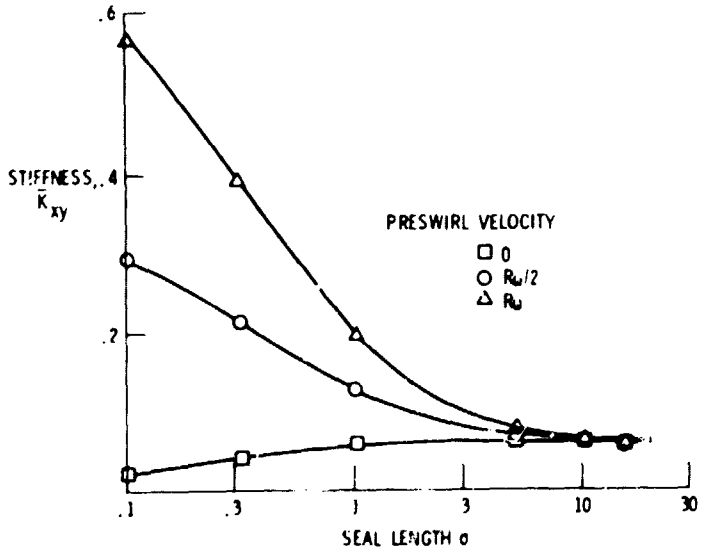

(b) Cross-coupled stiffness.

Figure 9. - Continued.

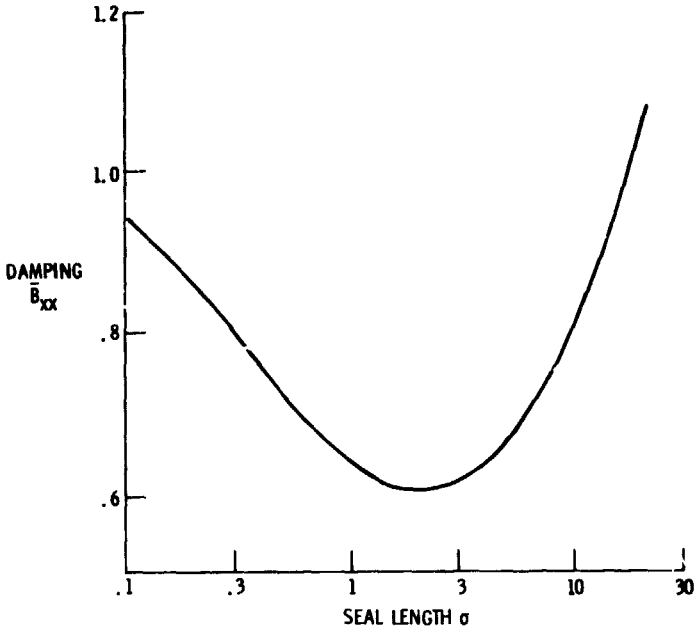

(c) Direct damping (all preswirl values).

Figure 9. - Continued.

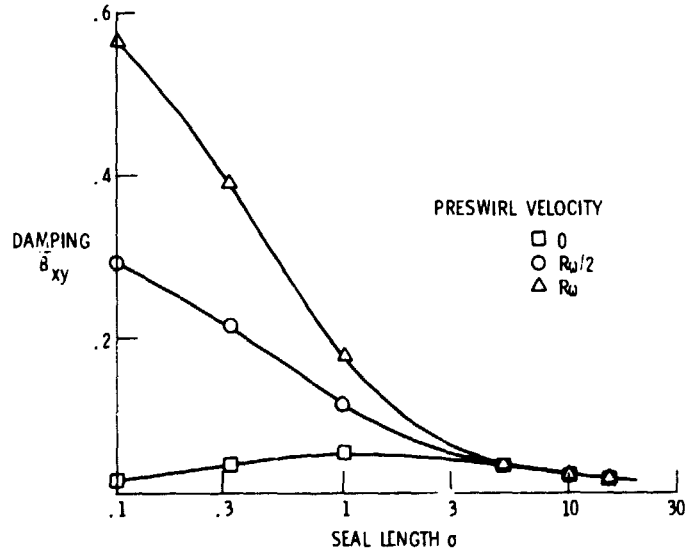

(d) Cross-coupled damping.

Figure 9. - Concluded.

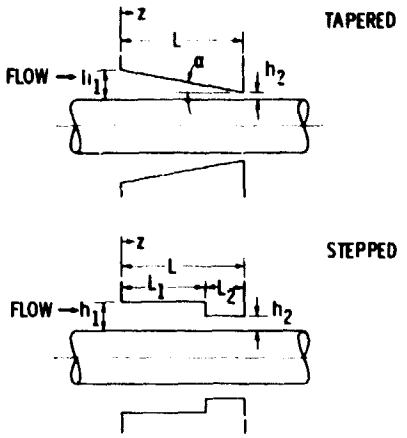

Figure 10. - Tapered and stepped annular seals.

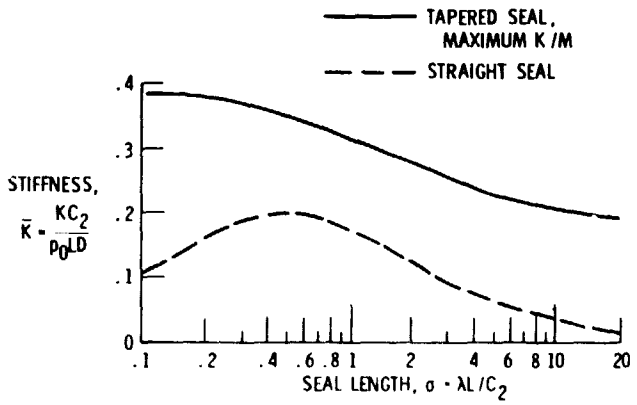

Figure 11. - Stiffness of tapered and straight seals.

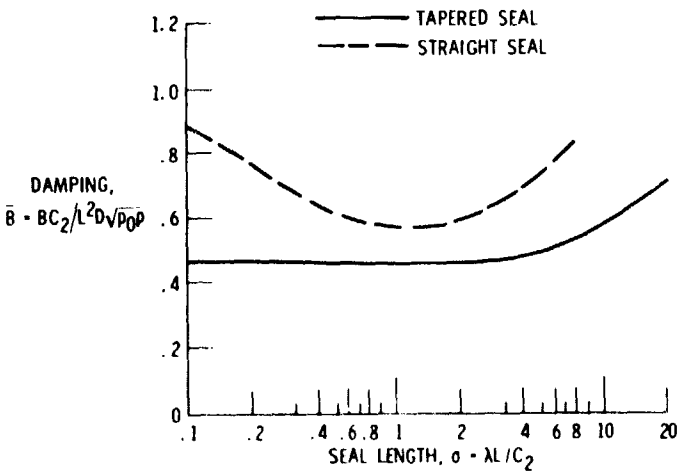

Figure 12. - Damping in tapered and straight seals.

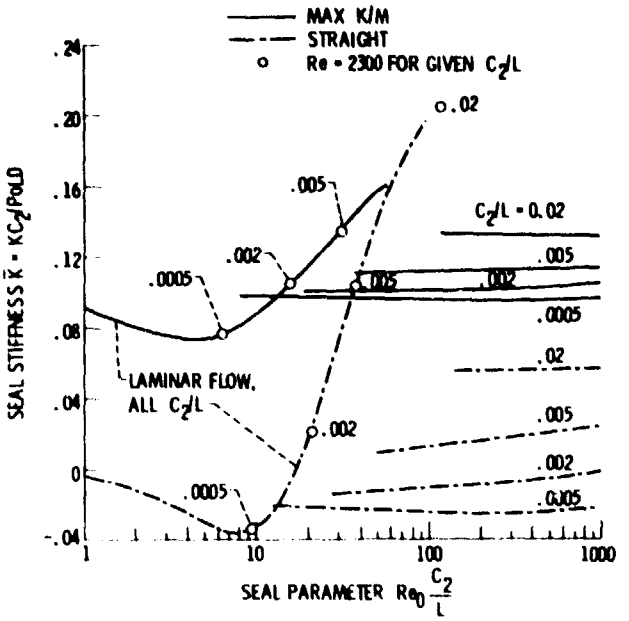

Figure 13. - Stiffness of straight and tapered seals; choked compressible flow.

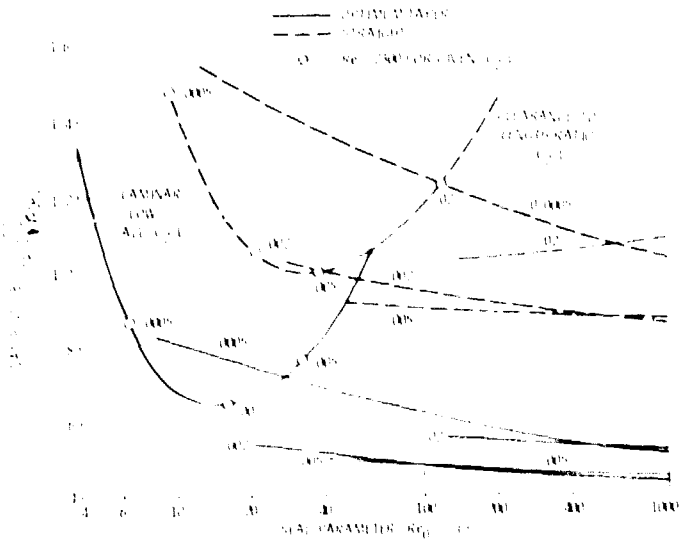

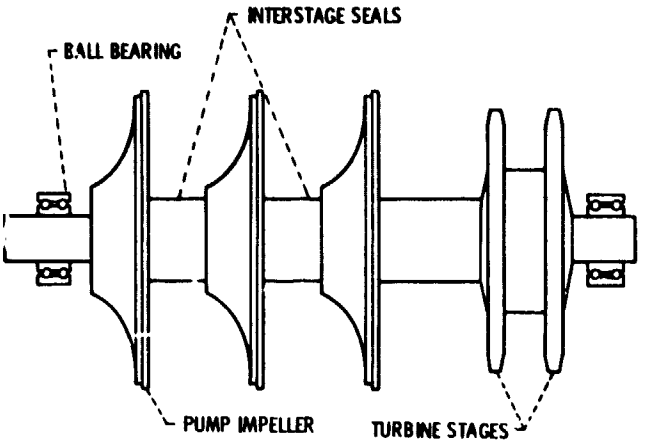

Figure 15. - Turbopump rotor.

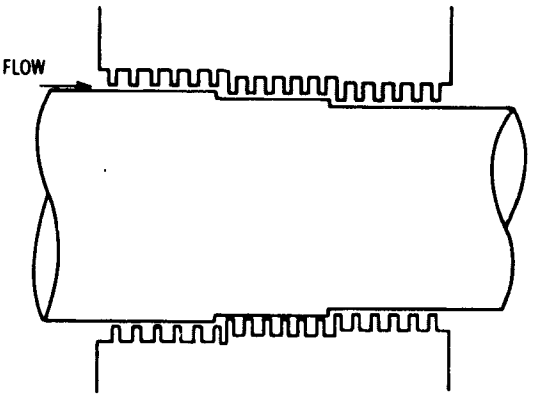

Figure 16. - Serrated seal.